The fast polarization modulation based dual-focus fluorescence correlation spectroscopy

Martin Štefl,[1,4] Aleš Benda,[1,3,4,*] Ingo Gregor,[2] and Martin Hof[1]

[1]*J. Heyrovsky Institute of Physical Chemistry, Academy of Sciences of the Czech Republic, v.v.i., Dolejškova 3, Prague 182 23, Czech Republic*

[2]*Georg-August-Universität Göttingen, 3rd Institute of Physics, Friedrich-Hund-Platz 1, D-37077 Göttingen, Germany*

[3]*Centre for Vascular Research and Australian Centre for NanoMedicine, University of New South Wales, Sydney, NSW 2052, Australia*

[4]*Authors contributed equally to this work*

[*]*a.benda@unsw.edu.au*

Abstract: We introduce two new alternative experimental realizations of dual focus fluorescence correlation spectroscopy (2fFCS), a method which allows for obtaining absolute diffusion coefficient of fast moving fluorescing molecules at nanomolar concentrations, based on fast polarization modulation of the excitation beam by a resonant electro-optical modulator. The first approach rotates every second linearly polarized laser pulse by 90 degrees to obtain independent intensity readout for both foci, similar to original design. The second approach combines polarization modulation of cw laser and fluorescence lifetime correlation spectroscopy (FLCS) like analysis to obtain clean correlation curves for both overlapping foci. We tested our new approaches with different lasers and samples, revealed a need for intensity cross-talk corrections by comparing the methods with each other and discussed experimental artifacts stemming from improper polarization alignment and detector afterpulsing. The advantages of our solutions are that the polarization rotation approach requires just one pulsed laser for each wavelength, that the polarization modulation approach even mitigates the need of pulsed lasers by using standard cw lasers and that it allows the DIC prism to be placed at an arbitrary angle. As a consequence the presented experimental solutions for 2fFCS can be more easily implemented into commercial laser scanning microscopes.

OCIS codes: (170.6280) Spectroscopy, fluorescence and luminescence; (180.1790) Confocal microscopy; (300.2530) Fluorescence, laser-induced.

References and links

1. D. Axelrod, D. E. Koppel, J. Schlessinger, E. Elson, and W. W. Webb, "Mobility measurement by analysis of fluorescence photobleaching recovery kinetics," Biophys. J. **16**(9), 1055–1069 (1976).
2. D. Magde, E. L. Elson, and W. W. Webb, "Fluorescence correlation spectroscopy. II. An experimental realization," Biopolymers **13**(1), 29–61 (1974).
3. N. L. Thompson, *Topics in Fluorescence Spectroscopy* (Plenum, 1991), pp. 337–378.
4. M. J. Saxton, "Single-particle tracking: effects of corrals," Biophys. J. **69**(2), 389–398 (1995).
5. P. Schwille, F. J. Meyer-Almes, and R. Rigler, "Dual-color fluorescence cross-correlation spectroscopy for multicomponent diffusional analysis in solution," Biophys. J. **72**(4), 1878–1886 (1997).
6. M. Böhmer, M. Wahl, H. J. Rahn, R. Erdmann, and J. Enderlein, "Time-resolved fluorescence correlation spectroscopy," Chem. Phys. Lett. **353**(5-6), 439–445 (2002).
7. Z. Petrášek and P. Schwille, "Precise measurement of diffusion coefficients using scanning fluorescence correlation spectroscopy," Biophys. J. **94**(4), 1437–1448 (2008).
8. R. Macháň and M. Hof, "Lipid diffusion in planar membranes investigated by fluorescence correlation spectroscopy," Biochim. Biophys. Acta **1798**(7), 1377–1391 (2010).

#200468 - $15.00 USD Received 30 Oct 2013; revised 16 Dec 2013; accepted 19 Dec 2013; published 8 Jan 2014

9. T. Dertinger, V. Pacheco, I. von der Hocht, R. Hartmann, I. Gregor, and J. Enderlein, "Two-focus fluorescence correlation spectroscopy: A new tool for accurate and absolute diffusion measurements," ChemPhysChem **8**(3), 433–443 (2007).
10. Y. Korlann, T. Dertinger, X. Michalet, S. Weiss, and J. Enderlein, "Measuring diffusion with polarization-modulation dual-focus fluorescence correlation spectroscopy," Opt. Express **16**(19), 14609–14616 (2008).
11. S. Felekyan, S. Kalinin, H. Sanabria, A. Valeri, and C. A. M. Seidel, "Filtered FCS: species auto- and cross-correlation functions highlight binding and dynamics in biomolecules," ChemPhysChem **13**(4), 1036–1053 (2012).
12. P. Kapusta, M. Wahl, A. Benda, M. Hof, and J. Enderlein, "Fluorescence lifetime correlation spectroscopy," J. Fluoresc. **17**(1), 43–48 (2007).
13. P. Kapusta, R. Macháň, A. Benda, and M. Hof, "Fluorescence lifetime correlation spectroscopy (FLCS): concepts, applications and outlook," Int. J. Mol. Sci. **13**(10), 12890–12910 (2012).
14. K. Akashi, H. Miyata, H. Itoh, and K. J. Kinosita, Jr., "Preparation of giant liposomes in physiological conditions and their characterization under an optical microscope," Biophys. J. **71**(6), 3242–3250 (1996).
15. A. Benda, V. Fagul'ová, A. Deyneka, J. Enderlein, and M. Hof, "Fluorescence lifetime correlation spectroscopy combined with lifetime tuning: New perspectives in supported phospholipid bilayer research," Langmuir **22**(23), 9580–9585 (2006).
16. J. Kriegsmann, I. Gregor, I. von der Hocht, J. Klare, M. Engelhard, J. Enderlein, and J. Fitter, "Translational diffusion and interaction of a photoreceptor and its cognate transducer observed in giant unilamellar vesicles by using dual-focus FCS," ChemBioChem **10**(11), 1823–1829 (2009).
17. C. T. Culbertson, S. C. Jacobson, and J. Michael Ramsey, "Diffusion coefficient measurements in microfluidic devices," Talanta **56**(2), 365–373 (2002).
18. A. Filippov, G. Orädd, and G. Lindblom, "The effect of cholesterol on the lateral diffusion of phospholipids in oriented bilayers," Biophys. J. **84**(5), 3079–3086 (2003).
19. K. Weiss and J. Enderlein, "Lipid diffusion within black lipid membranes measured with dual-focus fluorescence correlation spectroscopy," ChemPhysChem **13**(4), 990–1000 (2012).
20. A. Benda, M. Benes, V. Marecek, A. Lhotsky, W. T. Hermens, and M. Hof, "How to determine diffusion coefficients in planar phospholipid systems by confocal fluorescence correlation spectroscopy," Langmuir **19**(10), 4120–4126 (2003).
21. T. Dertinger, A. Loman, B. Ewers, C. B. Müller, B. Krämer, and J. Enderlein, "The optics and performance of dual-focus fluorescence correlation spectroscopy," Opt. Express **16**(19), 14353–14368 (2008).
22. J. Enderlein and I. Gregor, "Using fluorescence lifetime for discriminating detector afterpulsing in fluorescence-correlation spectroscopy," Rev. Sci. Instrum. **76**(3), 033102 (2005).

1. Introduction

Determination of diffusion coefficients in live cells or in model systems is usually achieved by fluorescence based methods like Fluorescence Recovery After Photobleaching (FRAP) [1], Fluorescence Correlation Spectroscopy (FCS) [2] [3] or fluorescence Single Particle Tracking (SPT) [4]. These methods are highly complementary, each exploring different concentration, spatial and also time ranges. A strong feature of FCS is its concentration range mostly suiting molecules abundance under cellular conditions (micromolar to nanomolar concentrations) and its coverage of long time span from nanoseconds to seconds. There exist multitudes of different realizations of FCS experiments, from simple fixed single focus single color FCS, through fixed multi-color [5] and lifetime FCS [6] or scanning FCS variants [7] to image correlation approaches like Raster Image Correlation Spectroscopy (RICS) [8]. Each variant suits different sample and experimental conditions. For studies requiring precise artifact free determination of diffusion coefficients (D) of small and middle size molecules freely diffusing in solvent ($D = 10^{-10} – 10^{-13}$ m^2s^{-1}) or laterally diffusing within a lipid membrane ($D = 10^{-12} – 10^{-13}$ m^2s^{-1}), dual-focus FCS is certainly the method of choice.

Dual-focus Fluorescence Correlation Spectroscopy (2fFCS) has become a very robust tool for determining absolute values of diffusion coefficients of fluorescent species in dilute solutions [9]. Its robustness comes from the introduction of an external ruler – a precisely known distance between two foci, which is insensitive to various aberrations coming from both the microscope and the measured sample. It has been shown that 2fFCS allows for precise determination of diffusion coefficients under strongly varying experimental conditions (temperature, refractive index of media, focal plane position alterations), where standard approaches fail [9].

#200468 - $15.00 USD Received 30 Oct 2013; revised 16 Dec 2013; accepted 19 Dec 2013; published 8 Jan 2014

The key aspect of 2fFCS is to have two overlapping foci, but still being able to distinguish fluorescence emitted from each of them. The standard approach [9] uses two pulsed interleaved lasers with crossed polarizations, which after passing a differential interference contrast (DIC) prism create two spatially overlapping, but time separated foci. The first attempt to simplify the hardware requirements for 2fFCS used an excitation beam polarization modulation at 100 kHz frequency, allowing for using cw lasers without the need of Time-Correlated Single Photon Counting (TCSPC) electronics [10]. The rather low frequency polarization modulation does not allow to separate intensity from both foci and instead of fitting clean auto- and cross- correlation functions for both foci a single auto-correlation curve is fitted by a more complex model accounting for the modulated mixing of auto- and cross-correlations.

In this contribution we demonstrate two new approaches, based on utilization of fast 20 MHz electro-optical modulator (EOM), to experimentally perform 2fFCS measurement. The first polarization rotation approach uses EOM to rotate polarization of every second laser pulse by 90 degrees, allowing 2fFCS setup with only one pulsed laser of each color. The second polarization modulation approach combines EOM polarization modulation of a cw laser with filtered fluorescence correlation analysis (filtered-FCS) [11], which can be considered as a generalized version of fluorescence lifetime correlation spectroscopy (FLCS) [12,13]. The polarization modulation of cw excitation beam is transformed by a DIC prism into two different excitation patterns (harmonic waves mutually shifted by a halfwave) for each focus. Knowing these patterns filtered-FCS analysis allows for auto- and cross-correlation of fluorescence from both foci, giving the same type of data as the pulsed version of 2fFCS. We show that these new approaches give correct diffusion coefficients both for 3-D diffusion in solution and for 2-D membrane lateral diffusion.

The presented approaches have the potential of widespread utilization in commercial laser scanning confocal microscopes, as they require only slight modification of the excitation path, an insertion of a compact EOM element, and require just one pulsed laser instead of two for polarization rotation approach, or even no pulsed laser at all, using only standard cw lasers, for polarization modulation approach.

2. Materials and methods

2.1 Materials

1,2-dioleoyl-*sn*-glycero-3-phosphocholine (DOPC), 1,2-dioleoyl-*sn*-glycero-3-phospho-(1'-*rac*-glycerol) (DOPG), cholesterol and 1,2-dipalmitoyl-*sn*-glycero-3-phosphoethanolamine-*N*-(cap biotinyl) (biotin-DPPE) were purchased from Avanti Polar Lipids (Alabaster, AL). *N*-(4,4-difluoro-5,7-dimethyl-4-bora-3a,4a-diaza-*s*-indacene-3-propionyl)-1,2-dihexadecanoyl-*sn*-glycero-3-phosphoethanolamine, triethylammonium salt (BODIPY® FL DHPE), Alexa Fluor® 488 NHS-ester, 5-carboxytetramethylrhodamine (5-TAMRA) and TetraSpeck™ microspheres (200 nm) were obtained from Invitrogen (Carlsbad, CA). Atto 425 with free carboxy group was obtained from ATTO-TEC (Siegen, Germany). Perylene, 5-carboxyfluorescein, streptavidin, biotin-labeled bovine serum albumin (BSA-biotin), 4-(2-Hydroxyethyl)piperazine-1-ethanesulfonic acid (HEPES), sodium chloride (NaCl), calcium chloride ($CaCl_2$), ethylenediaminetetraacetic acid (EDTA), glucose and sucrose were purchased from Sigma (St. Louis, MO).

2.2 Supported phospholipid bilayer (SPB) and giant unilamellar vesicle (GUV) preparation

SPBs: First, we prepared the mixture of appropriate lipids (final lipid concentration 2 mM), which contained the fluorescence dye in the lipid to dye ratio 200 000:1. The organic solvent was evaporated under the stream of nitrogen and thin lipid film was further kept for additional 2 h under the vacuum. The dried lipid film was subsequently hydrated with 10 mM HEPES buffer (150 mM NaCl, 1 mM EDTA, pH = 7.4) and the solution was extensively vortexed for

#200468 - $15.00 USD Received 30 Oct 2013; revised 16 Dec 2013; accepted 19 Dec 2013; published 8 Jan 2014

at least 2 min until multilamellar vesicles were formed. Next, the cloudy solution was sonicated for 20 min, yielding a solution of small unilamellar vesicles (SUVs). The SUVs were 10x diluted in the buffer containing Ca^{2+} ions (10 mM HEPES, 150 mM NaCl, 1 mM $CaCl_2$, pH = 7.4), moved to the cuvette with glass surface and incubated for 60 min. The redundant vesicles were flushed and the cuvette with SPBs was placed directly on the microscope objective and measured. The SPBs used in the measurements were composed of 75 mol% of DOPC and 25 mol% of cholesterol. The lateral diffusion of perylene (excitation 405 nm) and BODIPY® FL DHPE (excitation 470 nm) was monitored.

GUVs: GUVs were prepared by a gentle hydration method as described before [14]. 1 mL of desired lipids dissolved in chloroform and containing 1 mg of lipids was dried and placed under the vacuum for additional 2 h. Thin lipid film was hydrated with 3 mL of buffer (10 mM HEPES, 150 mM NaCl, 1 mM $CaCl_2$, 0.1 M sucrose, pH = 7). The tube was then sealed, heated up to 50 °C, kept overnight at this temperature, and slowly cooled down. White cloudy solution was gently vortexed before further use. All the prepared lipid mixtures contained 5 mol% of DOPG, negatively charged lipid necessary for the given preparation technique and 4 mol% of biotin-DPPE, which is needed for immobilization of GUVs to BSA-biotin/streptavidin coated glass surface. The BSA-biotin/streptavidin coated Lab-Tek chamber (NUNC A/S, Denmark) was filled with 380 μL of a buffer solution (10 mM HEPES, 150 mM NaCl, 1 mM CaCl2, 0.1 M glucose, pH = 7), 20 μL of the solution containing GUVs were added and after 30 min of incubation the measurements were performed. The GUVs were composed of 66 mol% of DOPC, 25 mol% of cholesterol, 5 mol% of negatively charged lipid DOPG and 4 mol% of biotin-DPPE. The lateral diffusion of BODIPY® FL DHPE (excitation 470 nm) was followed.

2.3 Experimental setup

All experiments were carried out on a home-built confocal microscope setup (Fig. 1) based on an inverted microscope body IX71 (Olympus, Japan). The setup contains two pulsed diode lasers (LDH405 and LDH470, driver unit 2-channel Sepia II, PicoQuant, Germany) and cw gas laser (HeNe 543 nm, Uniphase, Manteca, CA). Diode lasers offer <100 ps (FWHM) long pulses at up to 40 MHz repetition frequency with variable pulsing patterns, at wavelengths 405 nm and 470 nm. Diodes LDH405 and LDH470 can be also used in cw mode. Intensity of each diode laser is controlled via individual acousto-optical modulator AOM (MT200-A0.5-VIS and MQ110-A0.7-UV, AA OPTO-ELECTRONIC, France) allowing for fast (down to 10 ns for 470 nm, 1 us for 405 nm diode) intensity modulation without changing the pulse shape and/or frequency. The intensity of cw gas laser was controlled using a common acousto-optical tunable filter (AOTFnC-400.650-TN, AA OPTO-ELECTRONIC, France). All laser beams are overlapped using a set of dichroic mirrors (Semrock, NY). The combined beams with a vertical linear polarization enter into a resonant 20 MHz electro-optical modulator EOM (EO-AM-R-20-C4, Thorlabs, NJ) and are subsequently coupled into a single-mode polarization maintaining optical fiber (LINOS, Germany). The recollimation of laser beams at fiber output is done using a microscope objective (UPLSAPO 10x, Olympus, Japan). The collimated beam enters the back port of the microscope body and is reflected at the main dichroic mirror (Semrock, NY) through the inserted DIC prism (U-DICTHC, Olympus, Japan) into objective (UPLSAPO 60x/1.2 W, Olympus, Japan). The DIC prism is placed in a custom build holder and rotated by 45° compared to standard configuration. A 3D sample scanning is achieved by a compact three axis piezo stage (P-562.3CD driven by E-710.3CD, PI, Germany). The fluorescent light after passing through the main dichroic mirror is reflected into the left camera port and focused into 150 μm pinhole (Thorlabs, NJ) by internal microscope lens (180 mm focal length). The recollimated beam is equally split onto two APD detectors (PDM, MPD, Italy). Photon counting is performed by 2-channel HydraHarp 400 (PicoQuant, Germany), which is synchronized with pulsed diode lasers and EOM. Data are stored in time-tagged time resolved (TTTR) data format. Four channel

#200468 - $15.00 USD Received 30 Oct 2013; revised 16 Dec 2013; accepted 19 Dec 2013; published 8 Jan 2014

300 MHz PCI based Arbitrary Waveform Generator (DA4300-12-1M-PCI-10VPP, Acquitek, France) is used to drive the electro-optical (EO) crystal and to synchronize the phase modulation with laser pulsing, TTTR detection and laser intensity modulation. Additionally, a PCI based amplifier (AMP4100-PCI, Acquitek, France) is inserted in between the waveform generator and the EOM to reach proper voltage levels on the EOM input. An additional arbitrary waveform generator card (PCIe6259, National Instruments, TX) is used to modulate AOTF lines for cw lasers. The software for controlling the hardware and the acquisition process is written in LabVIEW (National Instruments, TX).

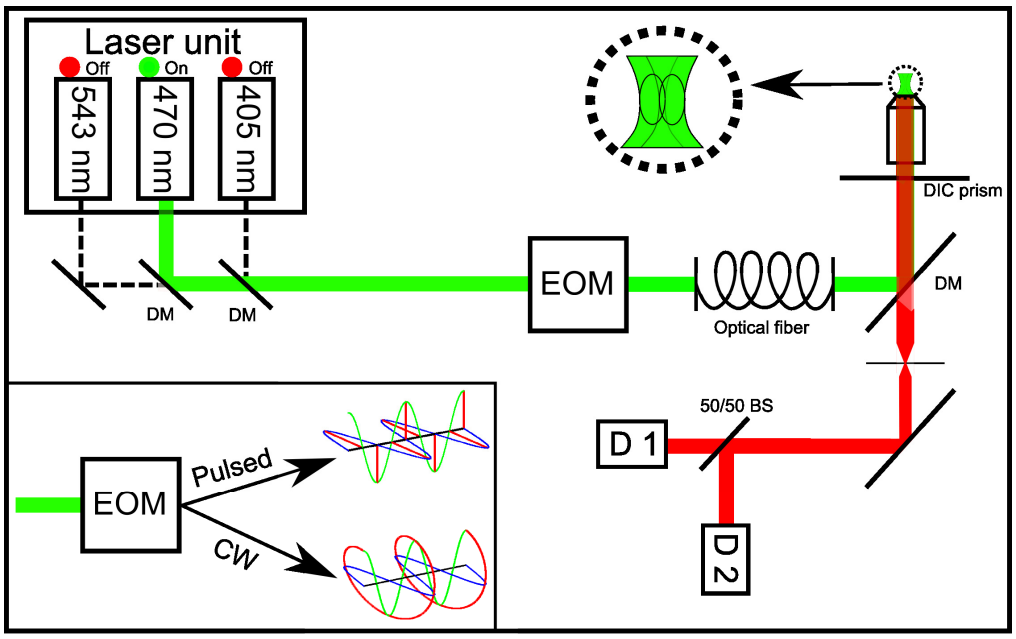

Fig. 1. Schematic illustration of the 2fFCS laser setup as modified in this contribution (DM corresponds to dichroic mirror). Inset: The EOM crystal periodically modulates the polarization state of the laser beam. The pulsed excitation (red lines) is synchronized with minima and maxima of polarization amplitudes for vertical and horizontal polarizations (green and blue lines), which results in discrete horizontal and vertical polarized excitation pulsed. In case of cw excitation EOM produces time varying elliptically polarized light (red spiral).

2.4 Filtered FCS analysis

Filtered FCS (fFCS) is a more general term for mathematically identical fluorescence lifetime correlation spectroscopy (FLCS) [15]. The difference is that in case of FLCS the species are resolved based on differences in their excited state lifetime behavior, whereas in the more general case of filtered FCS the species are resolved based on their different patterns in multichannel detection. The different patterns also include different excited state lifetimes, but in addition to that they can also include spectral differences, anisotropy differences and excitation modulation differences.

Briefly at every time t, the fluorescence intensity $I_j(t)$ in each detection channel j is a linear combination of area normalized detection patterns p_j^k:

$$I_j(t) = \sum_{k=1}^{n} w^k(t)\, p_j^k \qquad (1)$$

where k stands for a particular emitter with a specific detection pattern, n is the number of different emitters with different detection patterns and $w^k(t)$ is the contribution of the k^{th} fluorescent species to the total fluorescence signal at time t.

#200468 - $15.00 USD Received 30 Oct 2013; revised 16 Dec 2013; accepted 19 Dec 2013; published 8 Jan 2014

Equation (1) is an over-determined set of linear equations provided the number of detection channels is higher than the number of different emitters. Assuming that the photon detection obeys a Poissonian distribution and applying singular value decomposition, the solution of the Eq. (1) can be written as follows:

$$w^k(t) = \sum_{j=1}^{N} f_j^k I_j(t) \tag{2}$$

where N is the number of detection channels and f_j^k is a discrete filter function, which is constructed from the area normalized detection patterns of the different fluorescence species and the total intensities of the compound signal in detection channels. Explicitly, f_j^k is given by:

$$f_j^k = \left(\left[\hat{M}^T \cdot diag \left\langle I_j(t) \right\rangle_t^{-1} \cdot \hat{M} \right]^{-1} \cdot \hat{M}^T \cdot diag \left\langle I_j(t) \right\rangle_t^{-1} \right)_{kj} \tag{3}$$

where the matrix elements are:

$$\hat{M}_{jk} = p_j^k \tag{4}$$

Finally, the intensity normalized correlation function of the k^{th} species with l^{th} species (for auto-correlation $k = l$, for cross-correlation $k \neq l$) is calculated as:

$$G^{kl}(\tau) = \frac{\left\langle w^k(t) w^l(t+\tau) \right\rangle_t}{\left\langle w^k(t) \right\rangle_t \left\langle w^l(t) \right\rangle_t} = \frac{\sum_{i=1}^{N} \sum_{j=1}^{N} f_i^k f_j^l \left\langle I_i(t) I_j(t+\tau) \right\rangle_t}{\sum_{i=1}^{N} \sum_{j=1}^{N} f_i^k f_j^l \left\langle I_i(t) \right\rangle_t \left\langle I_j(t) \right\rangle_t} \tag{5}$$

2.5 Cross-correlation analysis

The spatial cross-correlation function *g(t)* between two confocal detection volumes for a freely diffusing molecule in 3-dimensional system was described by Dertinger et al. [9] and is given by the general relation:

$$g(t,\delta) = g_\infty(\delta) + 2\varepsilon_1 \varepsilon_2 c \sqrt{\frac{\pi}{Dt}} \int_{-\infty}^{\infty} dz_1 \int_{-\infty}^{\infty} dz_2 \frac{\kappa(z_1)\kappa(z_2)}{8Dt + \omega^2(z_1) + \omega^2(z_2)} \exp\left[-\frac{(z_2 - z_1)^2}{4Dt} - \frac{2\delta^2}{8Dt + \omega^2(z_1) + \omega^2(z_2)} \right] \tag{6}$$

where ε_1 and ε_2 are the factors proportional to the overall excitation intensity and detection efficiency, c is the concentration of diffusing molecules, D is the diffusion coefficient, z corresponds to the direction along the optical axis, $\omega(z)$ and $\kappa(z)$ are the parameters of molecule detection function and δ is the distance between foci which is characteristic for each individual DIC prism and wavelength. In the planar system, the cross-correlation function is simplified to the equation [16]:

$$g(t,\delta) = g_\infty(\delta) + \frac{\pi \varepsilon^3 c}{4} \frac{1}{4Dt + \omega^2(z)} \exp\left(\frac{-\delta^2}{4Dt + \omega^2(z)} \right). \tag{7}$$

For data fitting, we have implemented (both in Matlab and LabVIEW) and slightly modified a routine provided to us by Prof. Jörg Enderlein. In case of an improper signal separation stemming from the two foci the obtained experimental auto- (G_{A1} and G_{A2}) and cross- (G_{C12} and G_{C21}) correlations are combinations of true auto- *g(t,0)* and cross- *g(t,δ)* correlations according to Eq. (8):

#200468 - $15.00 USD Received 30 Oct 2013; revised 16 Dec 2013; accepted 19 Dec 2013; published 8 Jan 2014

$$
\begin{aligned}
G_{A1} &= (1-l_1)^2 + l_1^2)g(t,0) + (2(1-l_1)l_1)g(t,\delta), \\
G_{A2} &= (1-l_2)^2 + l_2^2)g(t,0) + (2(1-l_2)l_2)g(t,\delta), \\
G_{C12} &= G_{C21} = ((1-l_1)l_2 + (1-l_2)l_1)g(t,0) + ((1-l_1)(1-l_2) + l_1 l_2)g(t,\delta)
\end{aligned} \tag{8}
$$

where l_1 and l_2 are the fractions of the leak signal from the other focus, respectively. In case that the leak is 2% for each signal ($l_1 = l_2 = 0.02$. Instead of 100% of the signal coming from one focus only 98% percent comes from the proper focus and 2% from the wrong focus), the experimental autocorrelation contains only 96.08% of true auto-correlation and 3.92% of true cross-correlation. To correct for this in fitting we measured the signal leakage by bead scanning and experimental curves were fitted by leakage corrected sums of true auto- and cross- correlations (Eq. (8)).

A critical parameter for precise absolute data fitting, due to its correlation with the diffusion coefficient estimation, is the distance δ between the two foci. There are two standard methods to determine the inter-foci distance. The first way, which was applied to our system, employs imaging of immobilized fluorescence beads separately for each polarization and, then, finding the distance between the centers of mass by fitting the obtained intensity profiles with a Gaussian distribution function. The second approach is to calibrate the interfocal distance by measuring a standard sample with a precisely known value of diffusion coefficient.

3. Results

3.1 2fFCS based on interleaved polarization rotation of pulsed laser beam

The first presented alternative realization of 2fFCS is based on rotating polarization state of a train of laser pulses using EOM in such a way that all laser pulses have linear polarization state, but successive laser pulses have orthogonal orientation, matching the optical axes of a DIC prism. This configuration achieves the same result as the standard setup using two pulsed lasers rotated by 90 degrees, with the advantage of using just one laser for every wavelength. The rest of the optical setup is equivalent, including the data analysis.

For purposes of pulsed dual-focus FCS it is needed to align EOM such that during the resonant sine wave modulation of the crystal there are times when the outcoming beam polarization is linear vertical and other times when it is linear horizontal. If short laser pulses are sent only at these proper times, a train of laser pulses with desired properties is obtained - linear polarization and pulse by pulse interleaved orientation from vertical to horizontal and back. For an ideal system of linearly polarized cw laser beam passing lossless through the resonant EOM, the time profile of excitation intensity in each of the foci ($I_{f1}(t)$ and $I_{f2}(t)$) can be described as:

$$
\begin{aligned}
I_{f1}(t) &= I_0 \cos^2\left(\frac{1}{2}\left(\alpha + \pi\frac{V_{\max}}{V_\pi}\sin\left(2\pi f\left(t-t_0\right)\right)\right)\right), \\
I_{f2}(t) &= I_0 \sin^2\left(\frac{1}{2}\left(\alpha + \pi\frac{V_{\max}}{V_\pi}\sin\left(2\pi f\left(t-t_0\right)\right)\right)\right)
\end{aligned} \tag{9}
$$

where I_0 is the total intensity of the laser beam before EO crystal, α is the zero voltage retardance of EO crystal, V_{max} is the amplitude of sinusoidal driving voltage for EO crystal, V_π is the halfwave voltage for a given wavelength, f is the frequency of sinusoidal driving voltage, t is the time and t_0 is the time offset.

The zero voltage retardance of EO crystal can be tuned by slight tilting of the crystal in respect to the laser beam. The tilt changes the length of the light path, which causes change in the outcoming beam polarization state. We discovered that the most convenient EOM alignment is to have the quarter-wave zero voltage retardance and the driving voltage amplitude equal to or slightly higher than a quarter-wave voltage for a given laser

#200468 - $15.00 USD Received 30 Oct 2013; revised 16 Dec 2013; accepted 19 Dec 2013; published 8 Jan 2014

wavelength. Without any voltage applied, the outcoming beam is circularly polarized. For either positive or negative maximum voltage peak the outcoming beam is linearly polarized and oriented vertically or horizontally, respectively. The intensity profiles in both foci are shown in Fig. 2(a).

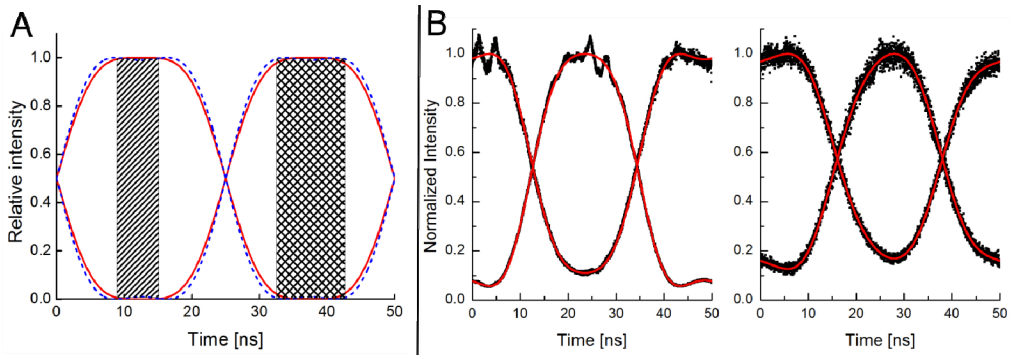

Fig. 2. (A) Theoretical time profile of excitation intensity in both foci (Eq. (9)) The red full lines show a time-profile for voltage amplitude equal to a quarter-wave voltage, the dotted blue lines for maximum plateau width voltage (1.128 times a quarter-wave voltage). The rectangles show time slots suitable for laser pulse positioning with less than 1% of cross-talk. The left rectangle is for a quarter-wave voltage and the right rectangle is for a maximum plateau width voltage. (B) Experimental time profiles of detected (B left) reflected light (diode laser 470 nm in cw mode) and (B right) fluorescence (Alexa 488) intensities for excitation polarized along both axes of DIC crystal. The experimental data are fitted by Eq. (10) (red lines). Fit parameters indicate that the zero voltage retardance of EO crystal is 0.62 ± 0.01, voltage amplitude is 0.79 ± 0.01 and Alexa 488 excited state lifetime 4.4 ns.

To test the performance of our system we measured intensity time profiles for reflected and fluorescence light with a polarizer placed in the excitation beam just before the dichroic mirror. The polarizer was sequentially aligned parallel with both optical axes of DIC prism to obtain intensity profile in each focus. For data fitting a constant intensity offset had to be added. This offset is caused by APD dark-countrate and afterpulsing. For the fitting of fluorescence profiles an excitation pattern is convoluted with fluorescence decay, resulting in equation (assuming a monoexponential decay):

$$F_{f1}(t) = F_0 + \left(I_0 \cos^2 \left(\frac{1}{2} \left(\alpha + \pi \frac{V_{\max}}{V_\pi} \sin\left(2\pi f \left(t - t_0\right)\right) \right) \right) \right) * e^{-t/t_1},$$
$$F_{f2}(t) = F_0 + \left(I_0 \sin^2 \left(\frac{1}{2} \left(\alpha + \pi \frac{V_{\max}}{V_\pi} \sin\left(2\pi f \left(t - t_0\right)\right) \right) \right) \right) * e^{-t/t_1}. \quad (10)$$

where F_0 is the constant offset, * identifies the convolution and t_1 is the excited state fluorescence lifetime. Fitted experimental data are shown in Fig. 2(b). Both the reflected and fluorescence light patterns for each focus can be satisfactorily fitted by using Eqs. (9) and (10), respectively. The obtained parameters describe the quality of the alignment, especially the zero voltage retardance of the EO crystal. The excited state fluorescence lifetime obtained from fitting the fluorescence pattern gives values of 4.4 ns for Alexa 488 in solution, a value close to 4.1 ns obtained by tail-fitting of standard TCSPC exponential decays. Employing the reflected light pattern in convolution improves the precision of the fit, giving an excited state lifetime of 4.15 ns.

#200468 - $15.00 USD Received 30 Oct 2013; revised 16 Dec 2013; accepted 19 Dec 2013; published 8 Jan 2014

Table 1. Diffusion coefficients for fluorescence standards in aqueous solution and lipid tracers in model bilayers (perylene (ex. 405 nm) and BODIPY FL DHPE (ex. 470 nm)). All values were achieved at 24°C. The error is expressed by standard deviation values (SD). * value corresponds to Atto488-carboxylic acid, ** value corresponds to Rhodamine B.

	Atto 425	Atto 488	Fluorescein	5-TAMRA
D [$\mu m^2 s^{-1}$]	438	426	452	489
SD [$\mu m^2 s^{-1}$]	90	19	23	30
Literature values	———	400* [17]	425 [17]	427** [17]
	SPBs (405nm)	**SPBs (470nm)**	**GUVs (470nm)**	
D [$\mu m^2 s^{-1}$]	5.8	3.8	13.5	
SD [$\mu m^2 s^{-1}$]	1.3	0.3	1.3	
Literature values	———	5.9 [18]	12.5 [19]	

3.2 Experimental determination of 3D- and 2D-diffusion coefficients using polarization rotation 2fFCS

To test the performance of polarization rotation 2fFCS experimental data were acquired for dyes freely diffusing in aqueous solution (Atto 425, Alexa 488 and carboxy-fluorescein, excitation wavelengths 405 nm, 470 nm and 470 nm, respectively) and for fluorescent markers (perylene and BODIPY® FL DHPE, excitation wavelengths 405 nm and 470 nm) laterally diffusing in lipid membranes of supported phospholipid bilayers (SPBs) or giant unilamellar vesicles (GUVs). For each pulsed 2fFCS measurement a TTTR photon stream was acquired for 10 minutes. The histogram of photon arrival times after 20 MHz EOM synchronization signal was decomposed into its components (fluorescence decays from excitation by vertical and horizontal polarization pulses plus a constant noise, Fig. 3(a)), from which the photon weighting filters were calculated (Fig. 3(c)) [12]. The auto- and cross-correlation functions were subsequently calculated using those weighting filters (Fig. 3(e)).

Diffusion coefficients of fluorescence dyes dissolved in water, and measured using various excitation wavelengths, are summarized in Table 1. The data are also compared with known literature values. Similarly, lateral diffusion coefficients of perylene in SPBs and of a labeled lipid analogue BODIPY FL DHPE in SPBs and GUVs, were determined and compared with closely related literature data. As seen from Table 1, our data do not significantly differ from literature values. Our experiments demonstrate that one EOM can be used with different laser wavelengths (405, 470 and 543 nm).

#200468 - $15.00 USD Received 30 Oct 2013; revised 16 Dec 2013; accepted 19 Dec 2013; published 8 Jan 2014

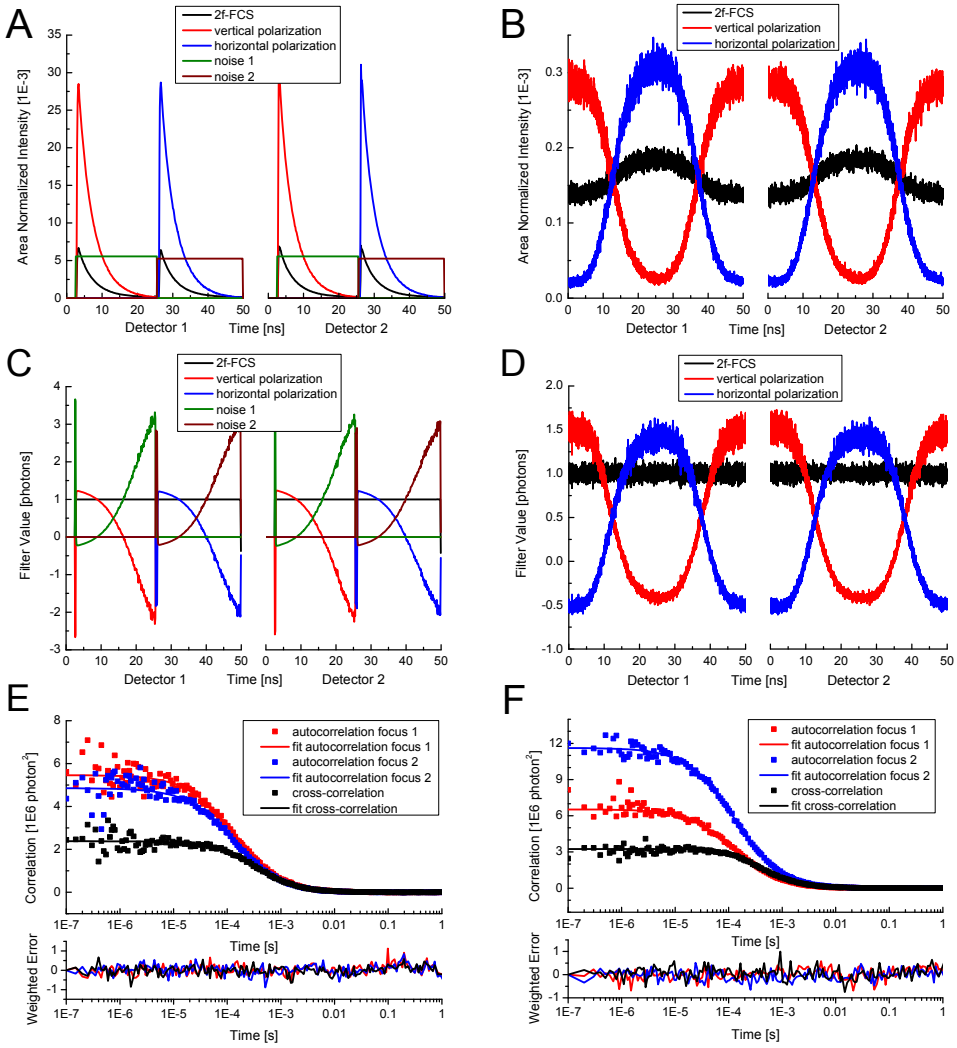

Fig. 3. Flowchart of data processing. (A) and (B) Area normalized histograms of photon arrival times for pulsed (A) and cw (B) acquisition (20 MHz sync frequency). The overall fluorescent signal (black line) is a linear combination of vertical polarization signal (red line), horizontal polarization signal (blue line) and of a constant afterpulsing and dark noise (green and brown). For cw excitation (B) the constant noise is a linear combination of vertical and horizontal polarization signal and cannot be separated. (C) and (D) Photon weighting filters for pulsed and cw acquisition, respectively, created from time resolved patterns (A) and (B). The sum of the patterns for each channel equals 1 (black line), keeping the overall intensity constant and showing that the overall signal is indeed a linear combination of the components. (E) and (F) Auto- and cross- correlation functions obtained by filtered correlation, globally fitted by Eq. (6), using the experimental standard error for weighting. Auto-correlation for focus 1 is obtained from vertical polarization filter, auto-correlation for focus 2 is obtained from horizontal polarization filter, and cross-correlation is obtained by cross-correlating filters for vertical and horizontal polarizations. Amplitudes of auto-correlations for different foci can differ due to different excitation light transmission efficiencies of vertically and horizontally polarized light through the optical system and the efficiency/sensitivity of detectors.

A very often discussed topic in the measurement of two-dimensional lateral diffusion by fluorescence correlation spectroscopy is the precise positioning of sample in the detection volume. Methods have been developed, which overcome those problems usually by sample scanning, which on the other hand implies a substantial increase in the measurement time.

#200468 - $15.00 USD Received 30 Oct 2013; revised 16 Dec 2013; accepted 19 Dec 2013; published 8 Jan 2014

One of such methods is z-scan FCS [20]. As already reported [21], lateral diffusion coefficient determination by 2fFCS is not sensitive to small nuances in axial position of the sample in the detection volume, which makes this method highly robust. To test our setup, point 2fFCS measurements on the membrane were performed at various axial positions of the detection volume for two different excitation wavelengths. Figure 4 shows lateral diffusion coefficients (D) in SPBs (Fig. 4(a)) and beam waist radii ω_0 (Fig. 4(b)) determined by polarization rotation 2fFCS analysis in dependence on the relative axial position in the detection volume. For both excitation wavelengths the beam waist radius decreases when approaching beam waist minimum and, then, increases when leaving the minimum. On the other hand, lateral diffusion coefficients remain constant for both 405 nm and 470 nm excitable dyes. The higher variability in lateral diffusion coefficients for 405 nm excitation is caused by a lower quality of the measured data, mainly stemming from a lower brightness of the used probe. To compensate for the lower brightness by a longer acquisition time is mainly limited by the z-axis stage drift and compensation by increasing the excitation power is limited by triplet state build-up and photobleaching of the probe. It is also worth noticing that perylene (a fluorescent membrane hydrophobic marker) diffuses in SPBs almost two-times faster in comparison to fluorescent lipid analogue (BODIPY FL DHPE).

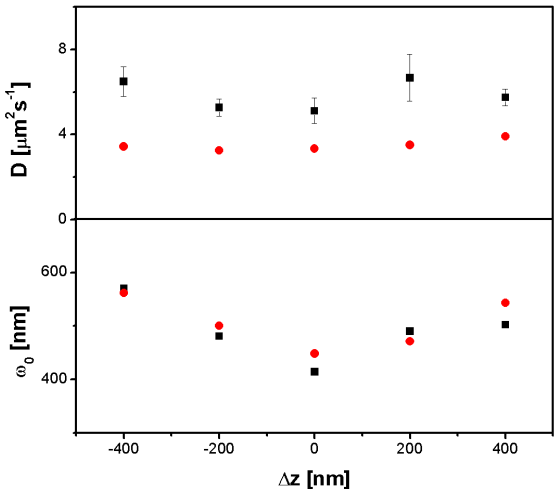

Fig. 4. (A) Lateral diffusion coefficients (D) determined for two different fluorescence dyes in SPBs, perylene (black squares) and BODIPY FL DHPE (red circles), in dependence on axial position in the detection volume. (B) Beam waist radii (ω_0) as determined from the analysis of 2fFCS data (405 nm black squares and 470 nm red circles). Each point at particular axial position corresponds to D in Fig. 4(a).

3.3 2fFCS based on polarization modulation of cw laser

The idea of the second presented alternative realization of 2fFCS is based on finding that it is not necessary to fully time-separate fluorescence photons coming from different foci to obtain clean auto- and cross- correlation functions for both foci. As has been demonstrated in Fluorescence Lifetime Correlation Spectroscopy [6] clean auto- and cross- correlation functions can be obtained from a linearly mixed signal of two (or multiple) components if their time-resolved emission patterns significantly differ. In typical FLCS analysis different diffusing species are resolved from a mixture due to differences in their fluorescence lifetimes (excited state decay patterns). The mixture of different contributors within a single confocal volume is excited by the same time profile of excitation pulse and their separation is based on time differences in their fluorescence response. The differences are usually caused by a different chemical structure or local environment.

#200468 - $15.00 USD Received 30 Oct 2013; revised 16 Dec 2013; accepted 19 Dec 2013; published 8 Jan 2014

In the case of 2fFCS there are no expected differences in excited state fluorescence lifetimes for fluorophores residing in either of the foci. In order to obtain different emission patterns for fluorophores having exactly the same emission properties, we must therefore excite them with a different excitation pattern. The difference between the two foci is their polarization. DIC prism splits the originally single beam with arbitrary polarization state into two slightly inclined beams with orthogonal linear polarizations. The creation of two inclined and collimated beams leads to the creation of two overlapping foci. The excitation intensity in each of the foci is directly related to the polarization state of the original single beam. A modulation of polarization state of the original beam is therefore transformed by the DIC prism into orthogonal excitation intensity modulations in both foci. By orthogonal it is meant that a relative intensity increase in one focus is complemented by an intensity decrease in the other focus. The difference in excitation profiles in each focus is then directly reflected in their different fluorescence emission patterns (Fig. 3(b)). As the intensity modulations are introduced by changing the polarization state using a fast 20 MHz EOM, there is no need for using a pulsed laser.

The fluorescence detection part is equivalent to the polarization rotation approach and uses the same hardware setup. Two SPAD channels signal is recorded by TTTR detection, which is synchronized with EOM modulation. As we use cw lasers here there is no need for laser synchronization. The modulated emission profiles are obtained by histogramming the arrival times of single photon detection events (TCSPC). An important difference comes in data analysis. The overall detected intensity at any given time is a linear combination of the contributions of both foci. To be able to use FLCS analysis for calculation of clean correlation functions, we need to know the emission pattern for each focus. The easiest way of obtaining the pattern for each focus separately is to insert a linear polarizer before the DIC prism. By turning the polarizer angle to sequentially match slow and fast axis of DIC prism it is possible to selectively excite fluorophores in one focus at time and record the emission patterns. The match of polarizer angle with optical axes of DIC prism is followed by taking images of fluorescent beads and optimizing the contrast between the two foci. All together there are three measurements needed for a polarization modulation 2fFCS (Fig. 3(b)). The first is the main measurement of diffusion with no polarizer inserted. The second is a measurement with a linear polarizer oriented along the fast axes of DIC prism and the third is a measurement with a linear polarizer oriented along the slow axes of DIC prism. The first main measurement usually takes several minutes to reach sufficient S/N ratio for correlation functions, whereas the patterns obtaining measurements can be fast, less than a minute. Combining these three measurements in FLCS analysis gives clean auto- and cross-correlation functions for both foci (Fig. 3(f)). These functions are theoretically identical to the correlation functions obtained from standard pulsed 2f-FCS. The polarization rotation of pulsed laser and polarization modulation of cw laser approaches differ in obtaining the correlation curves, but the subsequent curve fitting procedures are identical for both of them.

We demonstrated the polarization modulation 2f-FCS on aqueous solutions of Alexa 425, Alexa 488 and 5-TAMRA using continual 405nm, 470nm and 543nm excitation. First patterns from both foci were measured by placing the polarizer in front of the main dichroic parallel to optical axes of DIC prism. Afterward the polarizer was removed and the 2f-FCS measurement was performed (Fig. 3(b)). Mathematical filters were calculated from the known patterns and applied for correlation calculation (Fig. 3(d)). Resulting auto- and cross-correlation curves (Fig. 3(e)) were evaluated in standard way. Obtained diffusion coefficients are incorporated into Table 1. Quoted values are generated from polarization rotation measurements corrected for cross-talk and afterpulsing and polarization modulation measurements.

#200468 - $15.00 USD Received 30 Oct 2013; revised 16 Dec 2013; accepted 19 Dec 2013; published 8 Jan 2014

4. Discussion

4.1 Detectors afterpulsing in PIE cross-correlation experiments

Detector afterpulsing is a common drawback of many single photon counting detectors. In simple words the detector detects a ghost photon, which is not a real photon coming from the sample. The ghost photon appearance is related to the detection of the previous real photon, with a usual time delay on a microsecond time scale. The typical effect of the afterpulsing is a strong autocorrelation of the signal coming from a single detector on a microsecond time scale, which makes it difficult to analyze other fast processes, such as triplet state buildup, or even to properly fit fast diffusion components of autocorrelation curves. To avoid the afterpulsing contribution to the correlation curve usually a two detector setup is implemented, as is also done in standard 2fFCS setup and ours as well.

When analyzing our pulsed 2fFCS data we discovered another drawback of detector afterpulsing. So far pulsed interleaved excitation (PIE) experiments were considered cross-talk free. Photon arrivals are well separated on a nanosecond timescale and simple gating was used to get the signal from the first or the second laser pulse. This corresponds to obtaining a pure signal from green and red laser in a standard two color PIE experiment or for horizontal or vertical polarization in our 2fFCS case. Another problem that afterpulsing brings in is that the ghost photon is not anymore correlated to the laser pulse on a nanosecond timescale. It is correlated to the previous photon detection, but on a microsecond timescale, which causes the ghost photons to appear randomly distributed on a nanosecond timescale. Our detectors have up to 6% of afterpulsing, which can be seen as a constant background in the histograms. This background is added to the signal coming from single PIE pulses evenly during the gating approach. This means nothing else than that half of the ghost photons, in our case 3%, are attributed to the wrong pulse and cause a significant signal cross-talk, in our case 2.8%. The ghost photon is not related to the laser pulse, but is still related to the previous photon detection event, which in turn is related to the process happening in the sample (diffusion) and thus causes the cross-talk of the signals. This finding was confirmed by simple Monte-Carlo simulations of PIE experiment with afterpulsing (data not shown).

As has been just explained a simple time gating in PIE experiments is not sufficient to remove all afterpulsing artifacts in two-detector setup. Fortunately it is possible to remove the afterpulsing artifacts by FLCS [22]. The FLCS approach makes use of the uniform distribution of afterpulsing ghost photons, which allows them to be distinguished from real fluorescence photons and be simply filtered out during correlation. This approach was validated by our MC simulations (data not shown). In all our pulsed 2fFCS data analysis we solely used the FLCS approach to minimize the afterpulsing caused cross-talk. We suggest that FLCS afterpulsing removal should be a standard procedure for any type of PIE experiments.

4.2 Comparing polarization rotation of pulsed laser and polarization modulation of cw laser based 2fFCS

We have developed two new approaches for 2fFCS measurements. They differ in time profile and polarization modulation of the excitation beam and in data analysis, but they use the same optics. Theoretically both methods should give identical results. Since the 470 nm laser diode can be operated in both pulsed and cw mode, both methods were directly compared on aqueous solution of Alexa 488 yielding the correlation curves depicted in Fig. 5. It is apparent that the curves do not overlap, contrary to expectations. The differences can be explained by signal cross-talk. The non-ideal, real performance of optical elements involved in the microscope setup (dichroic mirror, DIC prism, mirrors) causes an improper separation of the excitation signal into the two foci. This improper signal separation leads to an apparent increase of relative cross-correlation amplitude (Fig. 5). It seems that the pulsed 2fFCS is more sensitive to the cross-talk than the modulated 2fFCS. This can be attributed to the fact

#200468 - $15.00 USD Received 30 Oct 2013; revised 16 Dec 2013; accepted 19 Dec 2013; published 8 Jan 2014

that the pulsed version assumes a complete time separation of the signals whereas the modulated version takes the separation as obtained from the real data. Without a cross-talk correction during the fitting procedure, one obtains artificially high diffusion coefficients or too short distance between foci. This trend is even more pronounced when exciting with 405 nm, due to a higher depolarization effect of the used optical elements at short wavelengths (data not shown). A proper correction, as described in methods, gives correct absolute values of diffusion coefficients and identical fit parameters for both pulsed and modulated 2fFCS.

The additional factor potentially affecting 2fFCS measurements is sample anisotropy. If the studied molecules cannot freely and fast reorient within the plane perpendicular to the optical axis, the amplitude of the cross-correlation would be lowered by a photo-selection effect as orientation of a fluorescence probe dipole along one excitation axis in the first focus would prevent excitation along the other axis in the second focus on the time scale of the relevant rotational time of the labeled molecules. In all the presented experiments this is not the case as the fluorophores can freely rotate on nanosecond and shorter time scale and their dipole orientation is symmetrical in respect to both excitation orientations.

4.3 Simultaneous multi-color 2f-FCS experiments

We have demonstrated that EOM based 2fFCS can be realized for different excitation (laser) wavelengths, both for the polarization rotation of pulsed laser and the polarization modulation of cw laser variant, using a single EOM element. As the amplitude of EOM driving voltage must be properly tuned for a given wavelength, properly aligned polarization rotation of two different wavelength laser pulses is not possible. Each pulsed laser has to have its own EOM. In case of polarization modulation of cw laser the EOM driving voltage amplitude is not

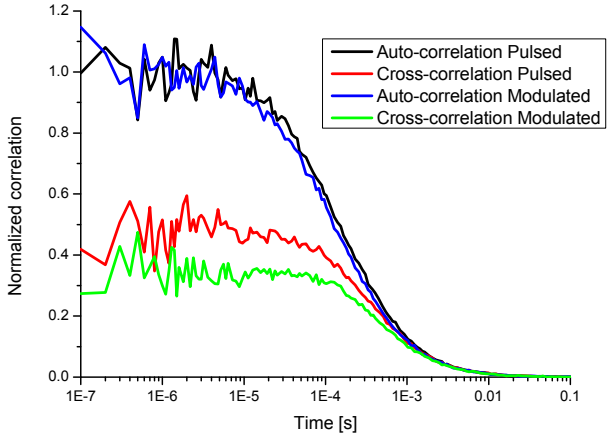

Fig. 5. Comparison of normalized correlation curves obtained by pulsed and modulated 2fFCS for Alexa 488 in aqueous solution. The small intensity cross-talk between foci for pulsed 2fFCS causes the resulting correlation curves to be a mixture of auto- and cross-correlations instead of being pure auto- or cross-correlations (Eq. (8)). This results in a longer apparent diffusion time for auto-correlation curve and a higher amplitude for cross-correlation curve compared to cross-talk free curves obtained by modulation 2fFCS.

critical. Important is that the time profiles of excitation for each focus (vertical and horizontal polarization) do differ and are known (measurable). Using two cw lasers of different wavelengths would result in different patterns for each wavelength and polarization. If the emission spectra of the two fluorophores are completely separated, two-color 2fFCS would be possible, using one detector for green and one detector for red emission. If the spectra overlap, causing a significant spectra cross-talk, there is no option to use filtering or gating to

#200468 - $15.00 USD Received 30 Oct 2013; revised 16 Dec 2013; accepted 19 Dec 2013; published 8 Jan 2014

remove the spectral crosstalk because the four involved emission patterns (red and green in horizontal and vertical polarization) are not orthogonal and cannot be used for data filtering.

The only option removing spectral cross-talk for simultaneous two color 2fFCS single EOM based acquisition is to combine polarization rotation of pulsed laser and polarization modulation of cw laser approaches. The EOM would be tuned for the wavelength of the pulsed laser, because the cw modulation approach is insensitive to the EOM driving amplitude. The acquired histogram of photon arrival times could be decomposed into four orthogonal patterns – two well separated pulses and two half wave shifted harmonic functions. The filtered correlation then should yield proper auto- and cross- correlations for each focus and wavelength.

5. Conclusion

We have shown that 2fFCS setups based on fast EOM polarization rotation and modulation are complementary tools to classical 2fFCS setup which uses two perpendicularly oriented linearly polarized pulsed lasers. Moreover, we have experimentally confirmed that our 2fFCS EOM polarization rotation and modulation setups are not limited to only one excitation wavelength, but can be used independently of the excitation wavelength. The inter-foci signal cross-talk, caused by imperfect optical elements and which has a negative impact on obtained data, was considered in the fitting routine and compensated for in data analysis. The measured amount of signal cross-talk in our setup is 3%. It was demonstrated that diffusion coefficients determined by the new setup for dyes excitable at different wavelengths (Atto 425 – 405 nm excitation, Alexa 488 and Carboxy-fluorescein – 470 nm excitation, TAMRA - 543 nm) are comparable to known literature values. The new approaches were also applied for lateral diffusion coefficients measurements in two model membrane systems (SPBs and GUVs) and for two excitation wavelengths (405 nm and 470 nm). Performing measurements in z-scan mode has shown that the obtained lateral diffusion coefficients are independent on axial membrane position within the detection volume, confirming the robustness of 2fFCS polarization rotation. Lastly we suggested and discussed limitations of possible experimental configurations for two color 2fFCS based on fast EOM polarization modulation.

Acknowledgments

We would like to thank Prof. Jörg Enderlein (Universität Göttingen) for providing us with 2fFCS curve fitting routine. A.B. acknowledges financial support from the Academy of Sciences of the Czech Republic (grant KJB400400904) and UNSW for VC's fellowship. M.Š. and M.H. acknowledge financial support from the Czech Science Foundation via grant P208/12/G016. Moreover, M.H acknowledges the Praemium Academie Award (Academy of Sciences of the Czech Republic).

#200468 - $15.00 USD Received 30 Oct 2013; revised 16 Dec 2013; accepted 19 Dec 2013; published 8 Jan 2014